

Alma Mater Studiorum Università di Bologna
Archivio istituzionale della ricerca

Focusing RF-on demand by logarithmic frequency-diverse arrays

This is the final peer-reviewed author's accepted manuscript (postprint) of the following publication:

Published Version:

Fazzini E., Al Shanawani M., Costanzo A., Masotti D. (2020). Focusing RF-on demand by logarithmic frequency-diverse arrays. Piscataway (NY) : Institute of Electrical and Electronics Engineers Inc. [10.1109/WPTC48563.2020.9295603].

Availability:

This version is available at: <https://hdl.handle.net/11585/794160> since: 2021-02-02

Published:

DOI: <http://doi.org/10.1109/WPTC48563.2020.9295603>

Terms of use:

Some rights reserved. The terms and conditions for the reuse of this version of the manuscript are specified in the publishing policy. For all terms of use and more information see the publisher's website.

This item was downloaded from IRIS Università di Bologna (<https://cris.unibo.it/>).
When citing, please refer to the published version.

(Article begins on next page)

This is the final peer-reviewed accepted manuscript of:

E. Fazzini, M. Shanawani, A. Costanzo and D. Masotti

Focusing RF-on demand by Logarithmic Frequency-Diverse Arrays

in: *2020 IEEE Wireless Power Transfer Conference (WPTC)*, 2020, pp. 76-79

The final published version is available online at:

<https://doi.org/10.1109/WPTC48563.2020.9295603>

Rights / License:

The terms and conditions for the reuse of this version of the manuscript are specified in the publishing policy. For all terms of use and more information see the publisher's website.

Focusing RF-on demand by Logarithmic Frequency-Diverse Arrays

Enrico Fazzini
Dept. Electrical, Electronic, and
Information Engineering
University of Bologna
Bologna, Italy
enrico.fazzini@studio.unibo.it

Mazen Shanawani
Dept. Electrical, Electronic, and
Information Engineering
University of Bologna
Bologna, Italy
mazen.shanawani@unibo.it

Alessandra Costanzo
Dept. Electrical, Electronic, and
Information Engineering
University of Bologna
Cesena, Italy
alessandra.costanzo@unibo.it

Diego Masotti
Dept. Electrical, Electronic, and Information Engineering
University of Bologna
Bologna, Italy
diego.masotti@unibo.it

Abstract—The radiating systems exploiting the frequency diversity of the antennas are powerful architectures, that can have a big impact on wireless power transmission applications, but their characterization is merely theoretical. This paper offers a deep and critical numerical analysis of frequency-diverse arrays and shows the advantages of the family with logarithmic distribution of the frequency for radio-frequency energy focusing goals. For the first time, these systems are analyzed through a Harmonic Balance-based simulation combined with the full-wave description of the array made of eight planar monopoles: the rigorous results confirm the potentialities of these complex radiating systems, in particular show how the time-dependency of the radiating mechanism can be favorably deployed.

Keywords—frequency diverse array, wireless power focusing, Harmonic Balance.

I. INTRODUCTION

Far-field wireless power transfer (WPT) is a widely studied topic and interesting practical applications has appeared in the literature [1] [2]. The main drawback of all these applications and also of the related theoretical studies is the poor efficiency of the overall system, mainly due to the lack of powerful transmitting architectures: the capability to point the transmitting narrow beam in a precise direction (where the target is placed) is possible with different and effective solutions: retrodirective arrays [3], leaky-wave arrays [2], or sophisticated time-modulated arrays [4] has already reached this goal. However, the capability of the target to capture the transmitted energy is very poor and this capability worsens with the increase of the covered distance.

For this reason, especially for future industrial Internet-of-Things (IoT) scenarios, there is an urgent need for radiating systems able to focus the energy in a precise spot of the space, thus selecting not only the angle, but also the distance at which the power must be sent. In this sense, one of the most promising family of arrays is represented by the frequency-diverse arrays (FDA), able to select both the direction and the range by means of the use of slightly different frequencies radiated by the array elements [5].

The complexity of these radiating systems makes the literature on FDA a theoretical speculation, up to now. A first attempt of realistic analysis of FDA has been proposed in [6]

for the simplest solution exploiting the frequency diversity, i.e., the uniform FDA. In this paper a deeper and critical analysis of arrays with a logarithmic frequency distribution (log-FDA) [7] is proposed and, for the first time, a realistic characterization of the time-dependency of the FDA radiation mechanism is given.

The simulation tool makes use of a joint combination of the Harmonic Balance technique [8] and of the full wave description of the array, given by a planar array of eight monopoles. Because of the complexity of the system under exam, an astute description of the nonlinear regime is adopted, thus making the simulations feasible on a standard PC.

II. FREQUENCY-DIVERSE ARRAYS FAMILIES

The exploitation of frequency diversity leads to very complex radiating architectures, whose accurate characterization can be a demanding task. Let us consider a linear array of M elements aligned along the x-axis, with d_m as the distance of the m-th element from the reference frame origin (here considered coincident with the phase center of the basis (0-th) antenna) and f_m its corresponding frequency given by:

$$f_m = f_0 + \Delta f_m \quad (1)$$

where f_0 is the radio-frequency (RF) carrier of the basis element.

Under these assumptions and the hypothesis of $f_0 \gg \max(\Delta f_m)$, the array factor (AF) in the far-field region ($r \gg \lambda$) can be cast in the following way:

$$AF(t, \theta, r) = \sum_{m=0}^{M-1} a_m \exp\left(j2\pi f_0 \left(\frac{d_m \sin(\theta)}{c}\right)\right) * \exp\left(j2\pi \Delta f_m \left(t - \frac{r}{c}\right)\right) \quad (2)$$

where c is the speed of light and a_m is the complex coefficient of the excitation current of the m-th element of the array. Except when explicitly underlined, $a_m = 1$ in the following.

A. Uniform FDAs

The uniform FDA (UFDA) is the simplest example of this array family: in this case the elements are equally spaced

($d_m = m \cdot d = m \cdot \lambda / 2$) and the Δf_m is a multiple of a constant frequency shift (Δf): $\Delta f_m = m \cdot \Delta f$. These radiating structures have been already described at circuit-level [6], but their limits in power focusing scenarios were not properly highlighted.

If we refer to Fig. 1, where the beam pattern (BP) (i.e., the square of (2)) of an 8-element UFDA is plotted in the case of $f_0 = 2.45$ GHz and $\Delta f = 10$ MHz, the S-shaped plot is clearly visible, as well as its space-periodicity: this means that the energy focusing capability is not univocal, i.e., when the array is pointing at $\theta = 40^\circ$, the power is focused around 10 m, but also around 40 m, and so on. Of course, this periodicity is a function of the frequency shift Δf , and can be a bit relaxed by decreasing it.

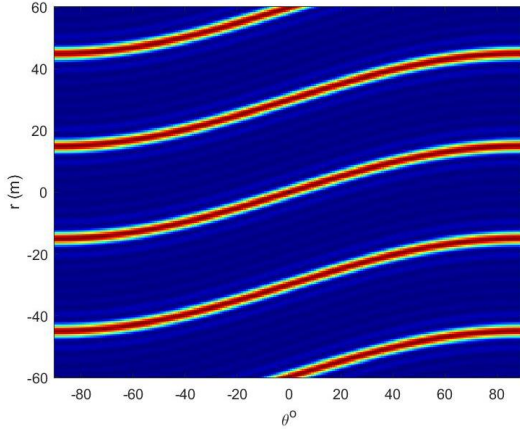


Fig. 1. Beam pattern in the (r, θ) space for a UFDA of 8 elements, with f_0 equal to 2.45 GHz and Δf equal to 10 MHz.

B. Logarithmically-spaced FDAs

An improvement of this behavior can be obtained by applying a logarithmic distribution of the spacing (d_m) between the elements [9]:

$$d_m = d * \log(m + 1) ; m = 0, \dots, M - 1 \quad (3)$$

where \log represents the natural logarithmic function and $d = \lambda / 2$.

However, the corresponding BP plot, even if more focused in space with respect to UFDA, offers the same space periodicity, as demonstrated in Fig. 2 (under the same excitation conditions of Fig. 1).

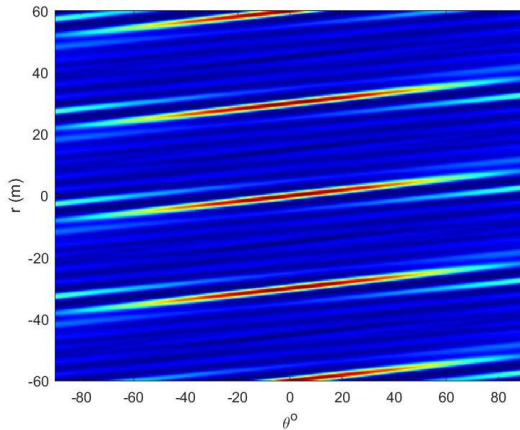


Fig. 2. Beam pattern in the (r, θ) space for a logarithmically-spaced FDA of 8 elements, with f_0 equal to 2.45 GHz and Δf equal to 10 MHz.

C. Logarithmic frequency-distributed FDAs

The best choice for energy-focusing applications is considered the (natural) logarithmic distribution of the frequency among the array elements, according to the simple rule [7]:

$$f_m = f_0 + \Delta f \log(m + 1) ; m = 0, \dots, M - 1 \quad (4)$$

The combination of the logarithmic distribution of both frequency and element spacing does not provide any added value with respect to the sole frequency distribution, and is not considered in the present work.

The BP plot in the case of log-FDA case is improved, because the space periodicity, even if not definitely eliminated, is significantly relaxed, as demonstrated by Fig. 3, again for of $f_0 = 2.45$ GHz and $\Delta f = 10$ MHz.

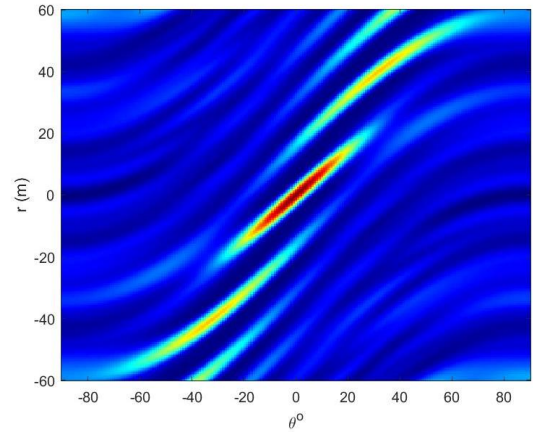


Fig. 3. Beam pattern in the (r, θ) space for a log-FDA of 8 elements, with f_0 equal to 2.45 GHz and Δf equal to 10 MHz.

The maximum spot of the AF is concentrated in a narrower region of the (r, θ) space. However, with respect to the UFDA case of Fig. 1, in this case the capability to point in a different θ direction is almost lost because of the missing S-shape of the plot.

For this reason, one possibility to have the maximum of the AF in a position different from $(r, \theta) = (0 \text{ m}, 0^\circ)$ is to play with the complex excitation coefficients a_m [7], thus increasing a lot the complexity of the already complex radiating architecture. However, if one can rely on modern software-defined radios (SDR), a specific phase condition at the antenna ports can be easily guaranteed: according to [7] the excitation coefficients have to obey to the following rule in order to focus the beam in the (r_{max}, θ_{max}) point:

$$a_m = \exp \left\{ j2\pi \left[\frac{\log(m+1) \Delta f r_{max}}{c} - \frac{f_0 m d \sin(\theta_{max})}{c} \right] \right\} \quad (5)$$

Another important issue of FDAs (in all their configurations) is the AF (and BP) time-dependency (see (2)): in fact, the graphs of Figs. 1, 2, and 3 are given for $t = 0$ s. This aspect is often not clearly investigated in the literature, but represents a strategic point for practical FDAs exploitation. In Fig. 4(a) the plot of BP of Fig. 3 vs. time is provided (for a time window of 100 ns): again, the logarithmic distribution of

the frequency relaxes the space-periodicity, as demonstrated by the corresponding plot of a UFDA shown in Fig. 4(b) (a similar one can be obtained for the logarithmic-distributed FDA); the delicate issue is that the maximum of the energy travels in time: the major concern of log-FDA is that there is not a time periodicity because of the logarithmic distribution of the frequency. This means that the plot of Fig. 4(a) always tends to increase, without any repetition in time, and this aspect must be considered in practical WPT applications, as explained in the last section. Vice versa, UFDA and logarithmically spaced FDA, having a common frequency shift Δf among the elements, periodically repeat their time behavior (with periodicity $T=1/\Delta f=100$ ns, in this case) (see Fig. 4(b)).

In this paper this time behaviour is investigated at circuit-level for the first time.

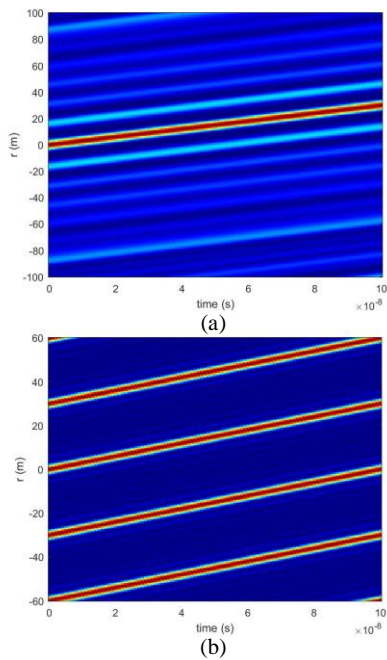


Fig. 4. Beam pattern vs. time for (a) a log-FDA, (b) a UFDA, both with 8 elements and f_0 equal to 2.45 GHz and Δf equal to 10 MHz.

III. FDA NUMERICAL CHARACTERIZATION

The numerical analysis of FDAs is a cumbersome problem, as already demonstrated in [6]. The situation becomes further complex in the log-FDA case under exam. In fact, a multi-tone (with M tones, one for each antenna) Harmonic Balance (HB) analysis [8] cannot be carried out because of the rapidly increasing number of intermodulation products that have to be taken into account.

A significant improvement is reached if a single-tone (i.e., periodic) analysis is carried out: for a UFDA the constant Δf is considered as the carrier frequency of the periodic regime and the excitation frequency of the different antennas are multiple of this basis frequency [6]. In the log-FDA case, a smaller least common multiple has to be adopted as carrier frequency, because of the not uniform frequency distribution. This will lead to: i) an error in the frequency definition of the array, but the impact can be negligible, as demonstrated in the last section; ii) a greater number of spectral harmonics with respect to the UFDA case: but the periodic nature of the regime (hence, the mono-dimensional nature of the Fast Fourier Transform and Inverse Fast Fourier Transform

algorithms adopted during the HB simulation) allows to manage hundreds of thousands of harmonics without high CPU time consumption.

Of course, from the far-field point of view, after the electromagnetic analysis of the array is performed, the extraction of the field pattern at the proper frequency for each antenna port must be carried out; after that, all the patterns are numerically combined after reaching the convergence of the HB analysis [6].

IV. LOG-FDA NUMERICAL RESULTS

As an example of log-FDA analysis, an array of 8 planar monopoles realized on a Rogers RO4360G2 substrate ($\epsilon_r=6.4$, $\tan\delta=0.0038$ and thickness=0.635 mm) is considered. The monopoles are equally spaced ($d=61$ mm= $\lambda/2$ @ 2.45 GHz) and the excitation frequencies are evaluated with (4) ($\Delta f=10$ MHz) and approximated in the following way: $f_0=2.45$ GHz, $f_1=2.4569$ GHz, $f_2=2.4610$ GHz, $f_3=2.4639$ GHz, $f_4=2.4661$ GHz, $f_5=2.4679$ GHz, $f_6=2.4695$ GHz, $f_7=2.4708$ GHz. The truncation of the results of (4) corresponds to a least common multiple of all the frequencies equal to 100 kHz: therefore, a periodic HB analysis with fundamental frequency $f=100$ kHz and 100,000 harmonics includes up to the fourth harmonic of the excitation frequencies, for nonlinear purposes.

The radiating architecture considers a single-FET amplifier (small-signal gain=15 dB) at each antenna port, as schematically described in Fig. 5.

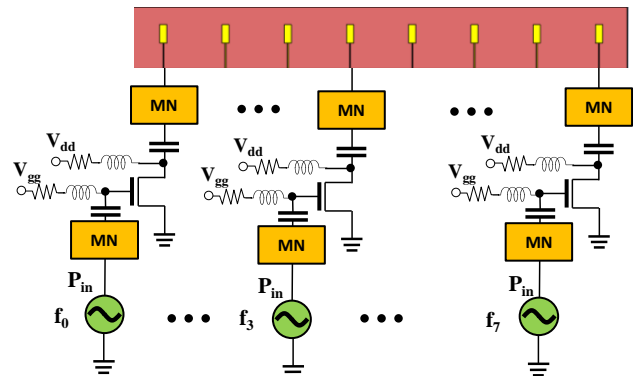


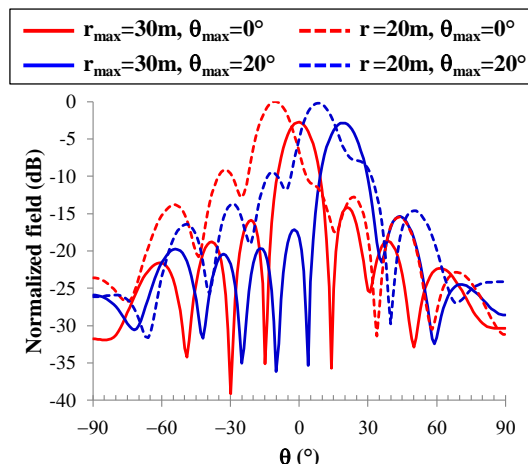
Fig. 5. Schematic view of the 8-monopole active log-FDA.

As a first analysis, the radiation patterns (at $t=0$ s) under non-uniform excitation conditions according to (5) are evaluated. First, for $(r_{max}, \theta_{max})=(30$ m, $0^\circ)$, then for $(r_{max}, \theta_{max})=(30$ m, $20^\circ)$. Each sinusoidal generator has (at its own frequency) an available power $P_{in} = -10$ dBm and the phase, obtained from (5), reported in Tab. I.

TABLE I. PHASE CONDITIONS AT THE 8 INPUT PORTS

m	$(r_{max}, \theta_{max})=(30$ m, $0^\circ)$	$(r_{max}, \theta_{max})=(30$ m, $20^\circ)$
0	0°	0°
1	-110.3°	-171.9°
2	35.8°	-87.3°
3	139.4°	-45.3°
4	-140.2°	-26.5°
5	-74.5°	-22.3°
6	-19.0°	-28.4°
7	-29.1°	-41.8°

Fig. 6 shows the normalized radiation patterns (in dB) for the two desired spots (solid lines) and the ones corresponding to the same phase excitation, but at a lower distance ($r = 20$ m) not corresponding to r_{max} . The impact of the proper phase-



distance condition is clearly visible: the maxima at 20 m point in different θ direction than those of Tab. I, are just few dBs greater than those at 30 m, and the side lobes at 20 m are less than 10 dB lower than the main lobe.

Fig. 6. Normalized radiation patterns for the log-FDA of Fig. 5 with non-uniform phase excitations: desired patterns focusing at 30 m (solid lines), undesired patterns (without focusing) at 20 m (dashed lines).

As a second example, the log-FDA behaviour vs. time is considered. Through inspection of Fig. 4(a), the maximum of the array factor is around 10 m at $t=35$ ns, and around 20 m at $t=60$ ns: note that, in this case, a simpler uniform excitation condition for all the antenna ports is considered, hence a maximum in the $\theta = 0^\circ$ direction is always provided. The corresponding normalized radiation patterns provided by an HB analysis at the time instant of interest are reported in Fig. 7: the solid lines correspond to the desired patterns at the proper (r, t) combination (i.e., (10 m, 35 ns) and (20 m, 60 ns)); the dashed lines are those of the undesired radiation patterns at the distance of 20 m, but at $t = 0$ and 35 ns, instants at which no maxima are present at 20 m (see Fig. 4(a)). The shape and the strength of the desired patterns are sensibly better than the corresponding ones at the wrong time instant.

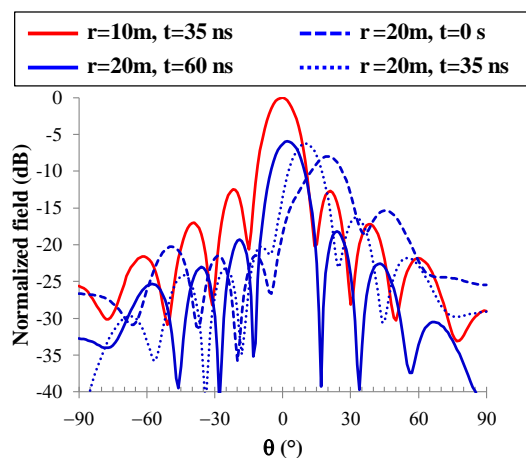


Fig. 7. Normalized radiation patterns for the log-FDA of Fig. 5 at different time instants and distances: desired patterns focusing at a given (r, t)

combination (solid lines), undesired patterns (without focusing) at wrong (r, t) combinations (dashed lines)

However, as previously said, the peculiarity of the log-FDAs is the lack of a periodicity in time of this radiation mechanism. This means that it is impossible to focus again at 10 or 20 m, if no countermeasures are taken: because of the possibility to create user-defined pulse as excitations at the array ports through modern SDRs, this fact does not represent a big concern. In practice, the time-periodicity can be imposed by switching off the system every Δt s and by applying a power pulse just before the switch-off. In this way, the time-dependency of these arrays can be favourably exploited: Δt becomes a further degree of freedom for the selection of the focusing range.

Moreover, if the non-uniform excitation condition is exploited, too, by changing both the excitation pulse position and the phase at the input ports any spot of the (r, θ) plane can be reached by a selective energy focusing operation. Additionally, also the Δf value can play the role of a design parameter.

A prototype realization is in progress, and the authors aim at driving the eight elements with a recently acquired SDR in a near future.

V. CONCLUSIONS

A deep investigation of the behaviour of FDAs with logarithmic distribution of the frequency has been presented. Despite of the complexity of their radiation mechanism, log-FDAs show promising selective focusing capabilities. The rigorous simulation tool here adopted, demonstrates that these capabilities, even if time-dependent, will be able to be favourably deployed in all WPT applications where the precise achievement of the target location is of paramount importance, such as in Industrial IoT scenarios.

REFERENCES

- [1] N. Shinohara, "History of Research and Development of Beam Wireless Power Transfer," *2018 IEEE Wireless Power Transfer Conference (WPTC)*, Montreal, QC, Canada, 2018, pp. 1-4.
- [2] M. Poveda-García, J. Oliva-Sánchez, R. Sanchez-Iborra, D. Cañete-Rebenaque and J. L. Gomez-Tornero, "Dynamic Wireless Power Transfer for Cost-Effective Wireless Sensor Networks Using Frequency-Scanned Beaming," in *IEEE Access*, vol. 7, pp. 8081-8094, 2019..
- [3] T. Matsumuro, Y. Ishikawa, M. Yanagase and N. Shinohara, "Both-Side Retrodirective System for Minimizing the Leak Energy in Microwave Power Transmission," *2018 Asia-Pacific Microwave Conference (APMC)*, Kyoto, 2018, pp. 780-781. 0.
- [4] D. Masotti, A. Costanzo, M. Del Prete and V. Rizzoli, "Time-Modulation of Linear Arrays for Real-Time Reconfigurable Wireless Power Transmission," in *IEEE Transactions on Microwave Theory and Techniques*, vol. 64, no. 2, pp. 331-342, Feb. 2016..
- [5] W. Wang, H. C. So and A. Farina, "An Overview on Time/Frequency Modulated Array Processing," in *IEEE Journal of Selected Topics in Signal Processing*, vol. 11, no. 2, pp. 228-246, March 2017.
- [6] D. Masotti, M. Shanawani, A. Costanzo, "Energy focusing through layout-based frequency-diverse arrays," *2019 IEEE Wireless Power Transfer Conference (WPTC)*, London, 2019, in press.
- [7] W. Khan, I. M. Qureshi and S. Saeed, "Frequency Diverse Array Radar With Logarithmically Increasing Frequency Offset," in *IEEE Antennas and Wireless Propagation Letters*, vol. 14, pp. 499-502, 2015.
- [8] V. Rizzoli, D. Masotti, F. Mastri and E. Montanari, "System-Oriented Harmonic-Balance Algorithms for Circuit-Level Simulation," in *IEEE Transactions on Computer-Aided Design of Integrated Circuits and Systems*, vol. 30, no. 2, pp. 256-269, Feb. 2011.

- [9] Y. Liao, W. Wang and H. Shao, "Symmetrical logarithmic frequency diverse array for target imaging," *2018 IEEE Radar Conference (RadarConf18)*, Oklahoma City, OK, 2018, pp. 0039-0042.